

VERIFICATION OF A CROSS-SHORE PROFILE MODEL USING FIELD DATA

Bart T. Grasmeijer¹, Leo C. Van Rijn², Steve Elgar³, Edith Gallagher⁴

ABSTRACT. A cross-shore process-based model was used to simulate the sediment transport rates near Egmond aan Zee, The Netherlands, and the morphological changes near Duck, NC, USA. Driven by the locally measured hydrodynamics and using a fixed bed roughness height of $r_w = 0.02$ m, the model predicted the current-related suspended transport rates near Egmond aan Zee within a factor 2 of the measured values, except for the very calm conditions. The wave-related transport rates were on an average a factor 4 smaller than the current-related components. The model was used to simulate calm weather waves with onshore bar migration and storm waves with offshore bar migration near Duck, NC. The morphological changes in the nearshore were primarily driven by cross-shore gradients in the current-related transport rate.

1. INTRODUCTION

In this paper we discuss the applicability of a numerical cross-shore model (CROSMOR) for the simulation of wave height, cross-shore undertow, longshore current, sand transport and morphological changes along an arbitrary cross-shore bed profile using data sets from two contrasting field sites: Egmond aan Zee, The Netherlands, and Duck, NC, USA.

The outline of the paper is as follows. First, the cross-shore model is described. Next, computed transport rates driven by locally measured wave heights and currents are compared with measured transports near the coast of Egmond aan Zee, The Netherlands. A comparison is made between measured and predicted hydrodynamics and morphological changes for two bar migration events near Duck, NC, USA. Finally, the findings are summarized.

¹ University of Utrecht, P.O. Box 80.115, 3508 TC, Utrecht, e-mail: B.Grasmeijer@geog.uu.nl

² Delft Hydraulics, P.O. Box 117, 2600 MH, Delft, e-mail: Leo.vanRijn@wldelft.nl

³ Woods Hole Oceanographic Institution, MS#11, Woods Hole, USA, e-mail: selgar@whoi.edu

⁴ Naval Postgraduate School, Monterey CA 93943, USA, e-mail: egallagh@oc.nps.navy.mil

2. MODEL DESCRIPTION

The cross-shore profile model is based on a wave-by-wave approach (Wijnberg and Van Rijn, 1996). This means that the propagation, transformation and breaking of individual waves are described by a probabilistic model. The individual waves shoal until an empirical criterion for breaking is satisfied. Wave height decay due to bottom friction and breaking is modeled by using an energy dissipation method. Wave-induced set-up and set-down and breaking-associated longshore currents are computed from the radiation stress gradients. The near-bed orbital velocities of the high-frequency waves are described by the method of Isobe and Horikawa (1982), which was modified by Grasmeijer and Van Rijn (1998) to be used with local wave conditions. Low-frequency wave effects are neglected. The depth-averaged return current under the wave trough of each individual wave is derived from linear mass transport and the water depth (h_t) under the trough. Streaming in the wave boundary layer due to viscous and turbulent diffusion of fluid momentum is also taken into account.

The sand transport rate of the model is determined for each wave class, based on the computed wave height, depth-averaged cross-shore and longshore velocities, orbital velocities, friction factors and sediment parameters. The net total sediment transport is obtained as the sum of the net bed load (q_b) and net suspended load (q_s) transport rates. The net bed-load transport rate is obtained by time-averaging (over the wave period) of the instantaneous transport rate using:

$$q_b = 0.5 \frac{D_{50} \rho_s U_* T}{D_*^{0.3}} \quad (1)$$

with D_{50} : median diameter [m]
 ρ_s : sediment density [kg/m^3]
 U_* : bed shear velocity [m/s]
 T : dimensionless bed shear stress [-]
 D_* : particle parameter [-]

The net suspended load transport is obtained as the sum ($q_s = q_{s,c} + q_{s,w}$) of the current-related and the wave-related transport components. The current-related suspended load transport ($q_{s,c}$) is defined as the transport of sediment particles by the time-averaged current velocities.

$$q_{s,c} = \int_a^h cu \, dz \quad (2)$$

The time-averaged concentration distribution is computed from the classical diffusion equation. The current-related mixing is derived from the standard expressions for turbulent flow. The wave-related mixing is described by an empirical expression based on data analysis. The sediment mixing near the bed depends on the bed roughness, and is related to the height of breaking waves. The near-bed reference concentration is computed from the excess bed shear stress and the relative wave height.

The wave-related suspended sediment transport ($q_{s,w}$) is defined as the transport of sediment particles by the oscillating fluid components (Grasmeijer et al. 1999):

$$q_{s,w} = k \int_a^h c \, dz * \frac{U_{on}^4 - U_{off}^4}{U_{on}^3 + U_{off}^3} \quad (3)$$

with a: reference height above the bed [m]
h: water depth [m]
c: time-averaged concentration [kg/m^3]
u: time-averaged velocity [m/s]
k: factor [-]
 U_{on} : peak onshore orbital velocity [m/s]
 U_{off} : peak offshore orbital velocity [m/s]
z: height above the bed [m]

The sand transport model can be used in the single fraction mode as well in the multi-fraction mode. The present computations are based on a single representative particle diameter (D_{50}).

3. VERIFICATION OF SAND TRANSPORT MODEL: EGMOND AAN ZEE

The data from the field site near Egmond aan Zee, The Netherlands, were obtained during two Coast3D field campaigns in April/May and September/October 1998 (Soulsby, 1998). The Egmond field site is situated south of the village of Egmond aan Zee along the Holland coast. The wave climate is dominated by wind waves. The tidal range near Egmond varies between 1.2 m (neap tide) and 2.1 m (spring tide). The semi-diurnal tide induces asymmetrical surface currents, which may reach values of 0.6 to 1.0 m/s. During the experiments the nearshore zone of the study area was characterized by two subtidal nearshore bars. The outer nearshore bar was located at 550m offshore. The inner nearshore bar at 200 m offshore (Figure 1). The sediments in the study area are well sorted and composed of fine to medium sand with a median grain size between 200 and 300 μm .

Measurements of wave height, velocity, and sediment concentration at four or five locations in a cross-shore array over the inner nearshore bar (Figure 1) were performed using the Coastal Research Instrumented Sledge (CRIS). Sand transport measurements were performed at eight elevations above the bed from 0.02 to 1.0 m. The instruments could be adjusted at a given elevation above the bed with an accuracy of ± 0.01 m using a vertically movable arm. The depth-integrated suspended transport rates ($q_{\text{suspension}}$) were determined using the measured time series of velocity and concentration. In the present paper the measured sediment transport rates are compared with computed sediment transport rates based on the measured hydrodynamics.

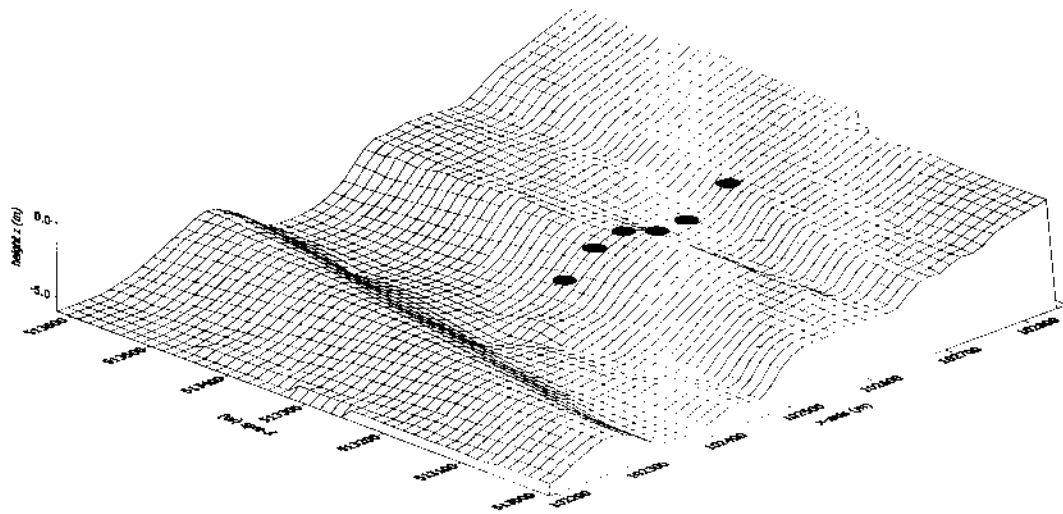


Figure 1. Example of nearshore morphology near Egmond aan Zee, The Netherlands, and CRIS positions across the inner nearshore bar on 9 April 1998.

The measurements were subdivided into classes according to their hydrodynamic conditions. Each class contains about 10 measurements and is represented by the peak onshore orbital velocity $U_{1/3,on}$. The computed concentrations and transport rates, based on the measured hydrodynamics, were also class-averaged to compare them with the measured values. Figure 2 shows the measured class-averaged concentration profile for $U_{1/3,on} = 0.50$ m/s and the computed profiles using different bed roughness heights. Generally, best comparison between the measured and computed values was found when using a bed roughness height of $r_w = 0.02$ m.

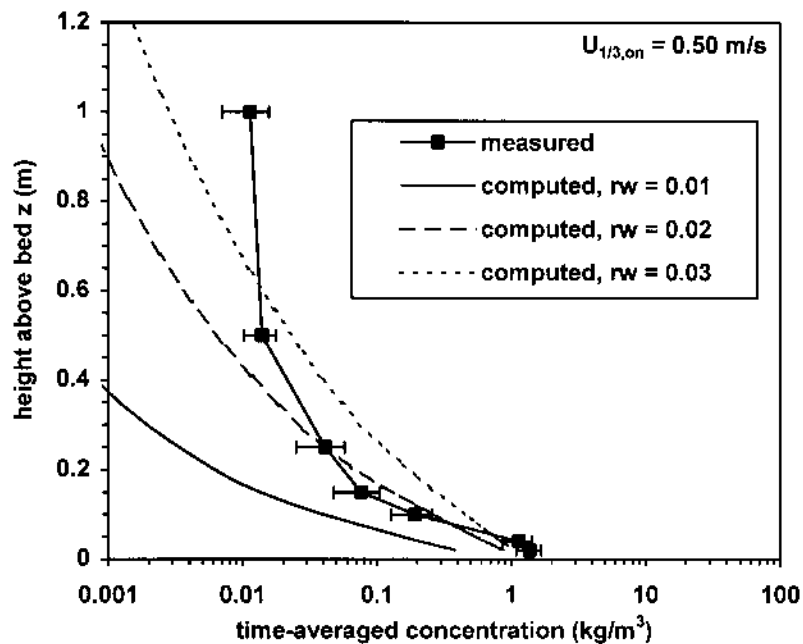


Figure 2. Measured and computed class-averaged concentration profiles ($U_{1/3,on} = 0.50$ m/s)

Figure 3 shows the measured and computed current-related suspended transport rates as a function of the peak onshore orbital velocity. A bed roughness height of $r_w = 0.02$ m was used. It can be seen that the model shows fairly good agreement with the measurements when using this fixed bed roughness height. The transport rates are slightly overestimated for large mobility values ($U_{1/3,on} > 1$ m/s) and underestimated for the calmer conditions ($U_{1/3,on} < 0.6$ m/s). This may be caused by the change in bed forms with increasing orbital velocity. It was observed in the measurements that the bed form generally changes from a rippled bed for small orbital velocities to flat bed or mega ripples for larger values. This effect is not incorporated in the model. Discrepancies between the model computations and the measurements may also occur because of the grading of sediment. The present computations are based on a single representative diameter. In case of multiple fractions the smaller particles are stirred up higher in the water column than the coarser ones, leading to larger concentrations and thus higher transport rates compared with the single fraction method. The multiple fraction method will be discussed in future studies. It is interesting to see that, except for the very calm conditions, using the single fraction method results in predictions that are within a factor 2 of the measured values.

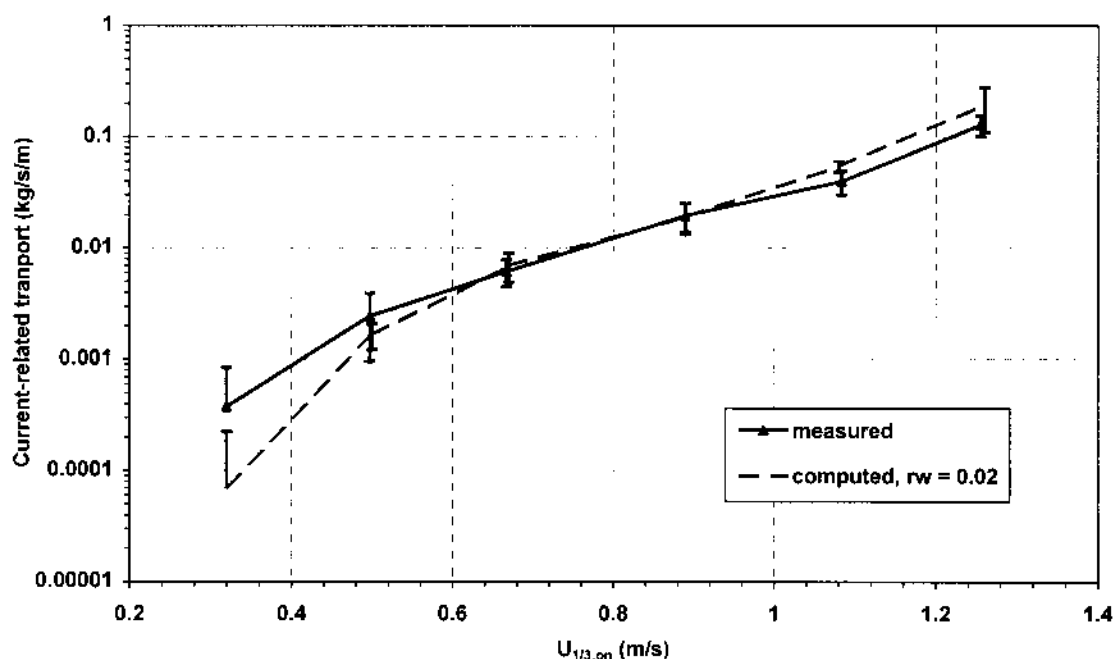


Figure 3. Measured and computed current-related suspended transport rates (class-averaged) near Egmond aan Zee, The Netherlands, as a function of the peak onshore orbital velocity.

The wave related transports are presented in Figure 4. Except for the very calm conditions ($U_{1/3,on} < 0.6$ m/s), the measured wave-related transport rates are between 2 and 10 times smaller than the measured current-related components. The computed wave-related transport rates, based on Equation 3 with efficiency factors $k = 0.05$ and 0.2 , are also shown in Figure 4. It can be seen from this figure that both k values lead to an overestimation of wave-related transport rates. An efficiency factor of $k = 0.02$ gave the best fit. Theoretically k would have a value of 0.44 but phase lags between

the velocity and concentration signal lead to smaller values. Field and laboratory experiments (Grasmeijer et al 1999, Houwman and Ruessink 1996) have shown that the efficiency factor lies in the range between $k = 0$ and 0.3. Another reason for the small efficiency factor may be that the sediment does not respond instantaneously to the third power of the velocity, which is implicitly assumed in this method (Grasmeijer et al, 1999).

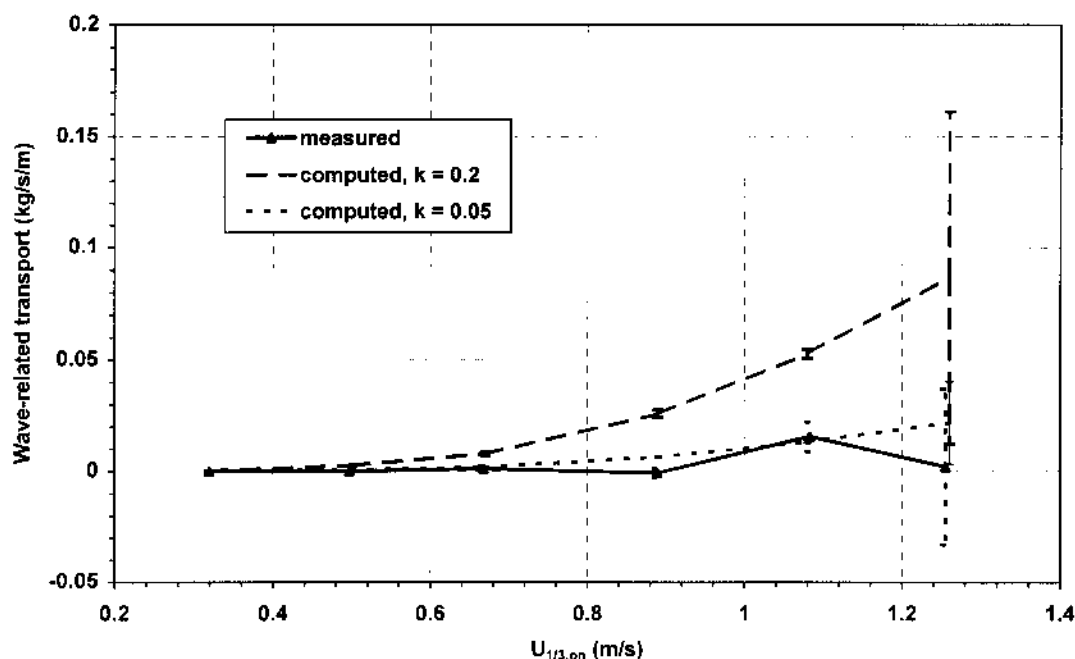


Figure 4. Measured and computed wave-related suspended transport rates (class-averaged) near Egmond aan Zee, The Netherlands, as a function of the peak onshore orbital velocity.

4. VERIFICATION OF CROSS-SHORE MORPHODYNAMIC MODEL: DUCK

The data from the field site near Duck, NC, USA, were obtained during the Duck94 field experiment in September and October 1994. The Duck field site is situated on the east (Atlantic) coast of the USA. The tidal range is about 1 m and the tidal currents are weak (0.1 to 0.3 m/s). The winter period is dominated by storm waves and the summer period is dominated by long-period swell. The bed profile generally shows a single bar in the surf zone (Figure 5) and sometimes a low outer bar is present. A description of the experimental set-up and of the nearshore bar behavior during the Duck94 measurement campaign is given by Gallagher et al (1998). The model was used to simulate calm weather waves with onshore bar migration in the period 21-26 September and storm waves with offshore bar migration in the period 10-20 October 1994.

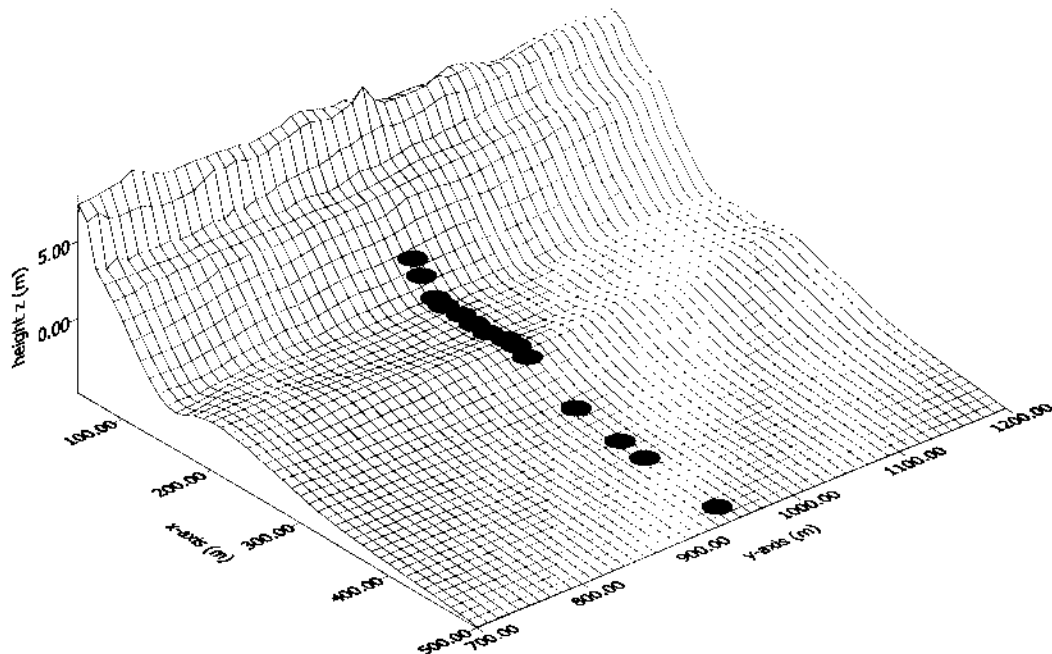


Figure 5. Example of local morphology near Duck, NC, USA, with location of instruments during the Duck94 experiments, 21 September 1994.

During the period September 21-26, the bar crest moved onshore over a distance of about 15 m. During this period a minor storm occurred on September 22 with a significant wave height of about 2.5 m at a position 800 m offshore. For the rest of time the conditions were relatively calm with wave heights between 0.5 and 1 m.

Figure 6 shows an example of the measured and computed hydrodynamics across the nearshore bar on 22 September 1994. The offshore significant wave height was about 1.9 m. The computed wave heights show very reasonable agreement with the measured values. The wave heights are about 20% overestimated near the bar trough. The measured longshore currents are fairly well represented by the model with exception of the offshore zone ($x < 100$ m). The measured cross-shore velocities show unexpected variations not seen in the model calculations. The measured and computed cross-shore current varies roughly between 0.0 and -0.2 m/s. It is noted that the measured currents are defined at about 0.5 m above the bed, whereas the computed values represent the depth-averaged currents.

Figure 7 shows the measured and computed cross-shore profile change between 21 and 26 September 1994. The measured profiles show erosion on the seaward flank and deposition on the landward flank of the bar resulting in an onshore migration over a distance of about 15 m. Two computations were made with $k = 0.2$ and 0.05 (Equation 3).

Using $k = 0.2$ the model shows slight onshore migration of the bar with some erosion in the trough and generation of an intertidal bar near the beach. The intertidal bar is not observed in the measured data. It is noted that swash processes are not incorporated in the model. Modelling the hydrodynamics and sand transport processes in this region near the beach needs further study. The model computation

using $k = 0.05$ (Figure 7) shows a flattening of the bar profile with no onshore migration and the generation of a small intertidal bar near the beach. In both computations a bed roughness height of $r_w = 0.03$ m was used for the region near the bar trough ($260 \text{ m} < x < 320 \text{ m}$) and $r_w = 0.02$ for other parts of the profile.

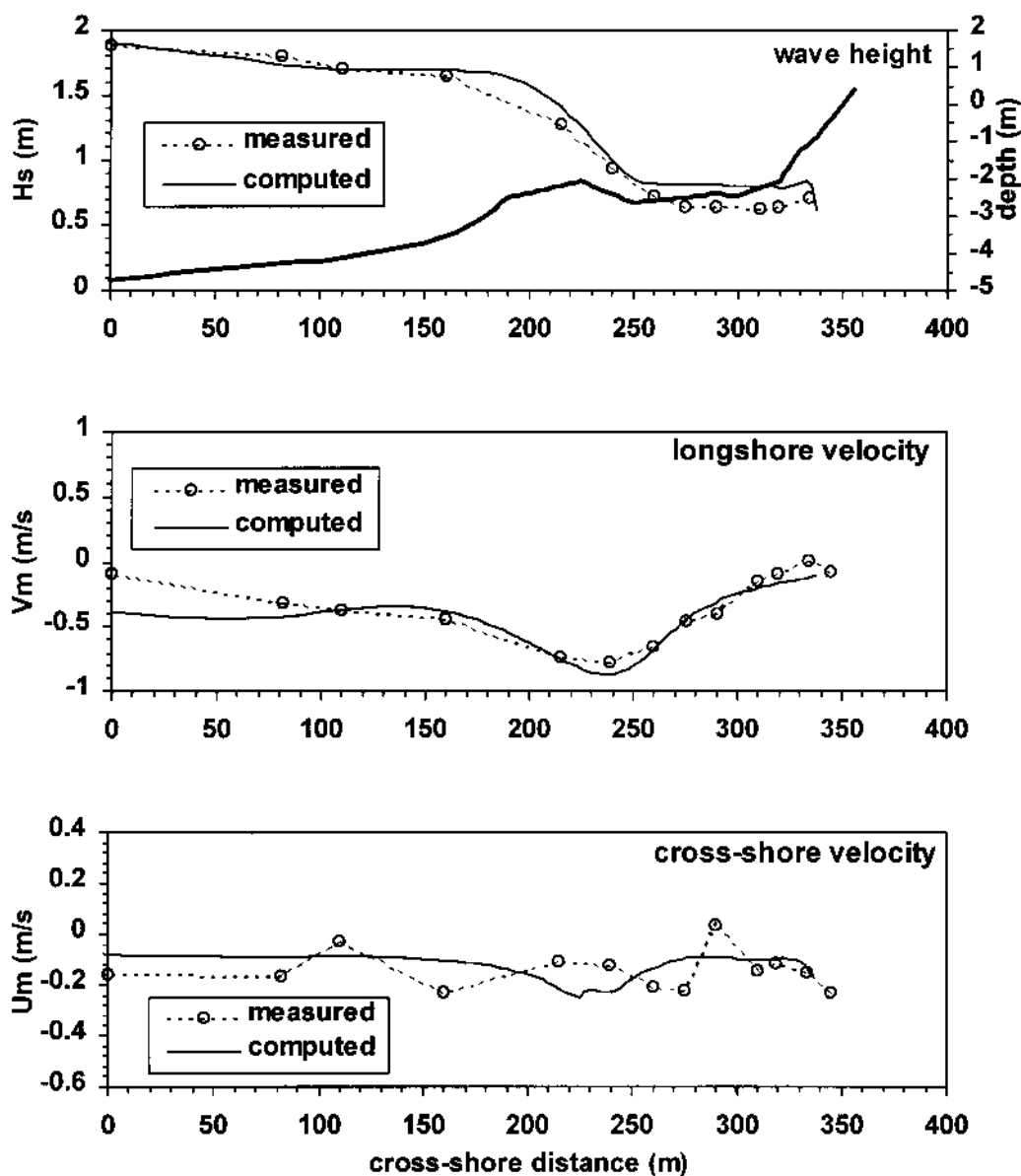


Figure 6. Example of measured and computed wave heights, time-averaged cross-shore and longshore velocities near Duck on 26 September 1994.

During the period October 10-20, the bar crest moved about 75 m in the offshore direction. The significant wave height during this period at a position 800 m from the shore varied between 0.5 and 4.0 m. Offshore migration occurred primarily during high-energy wave conditions. Slight onshore bar movement occurred during the calmer periods (see Gallagher et al, 1998).

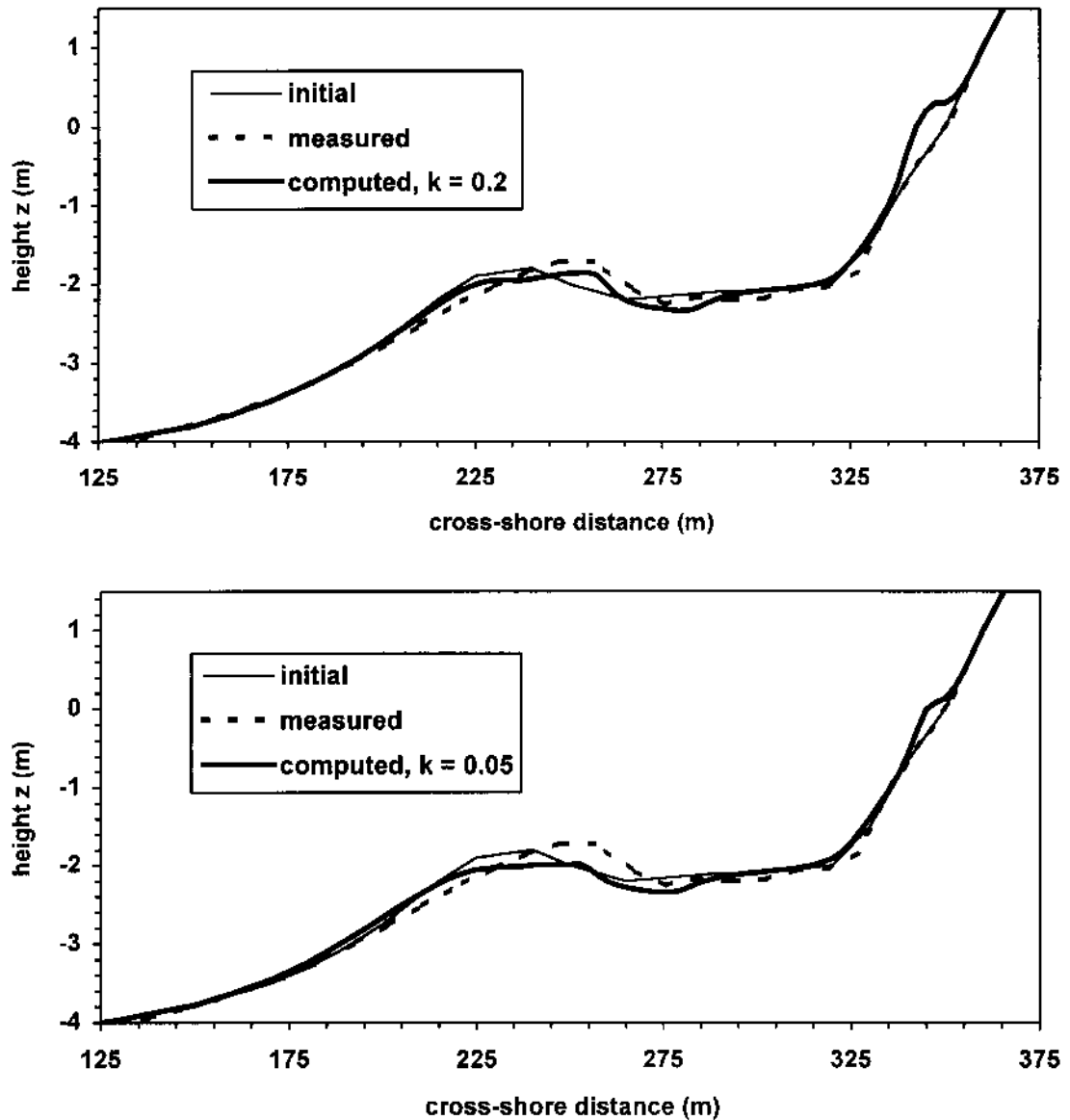


Figure 7. Measured and computed cross-shore profile changes near Duck from 21 to 26 September 1994.

Figure 8 shows an example of the measured and computed hydrodynamics across the nearshore bar on 14 October 1994. The offshore significant wave height was about 2.3 m. The computed wave heights show reasonable agreement with the measured values in the zone seaward of the bar. The modelled wave heights are about 20% too large in the region near the bar and landward of the bar. The longshore currents calculated with the model show a distinct peak just landward of the bar crest of about 1.0 m/s, which is in good agreement with measured values, although the peak seems to be located somewhat more landward in the measurements.

The measured cross-shore velocities show a strong peak of about -0.6 m/s just landward of the bar crest, whereas the maximum computed undertow velocity is -0.2 m/s and is located just seaward of the bar crest.

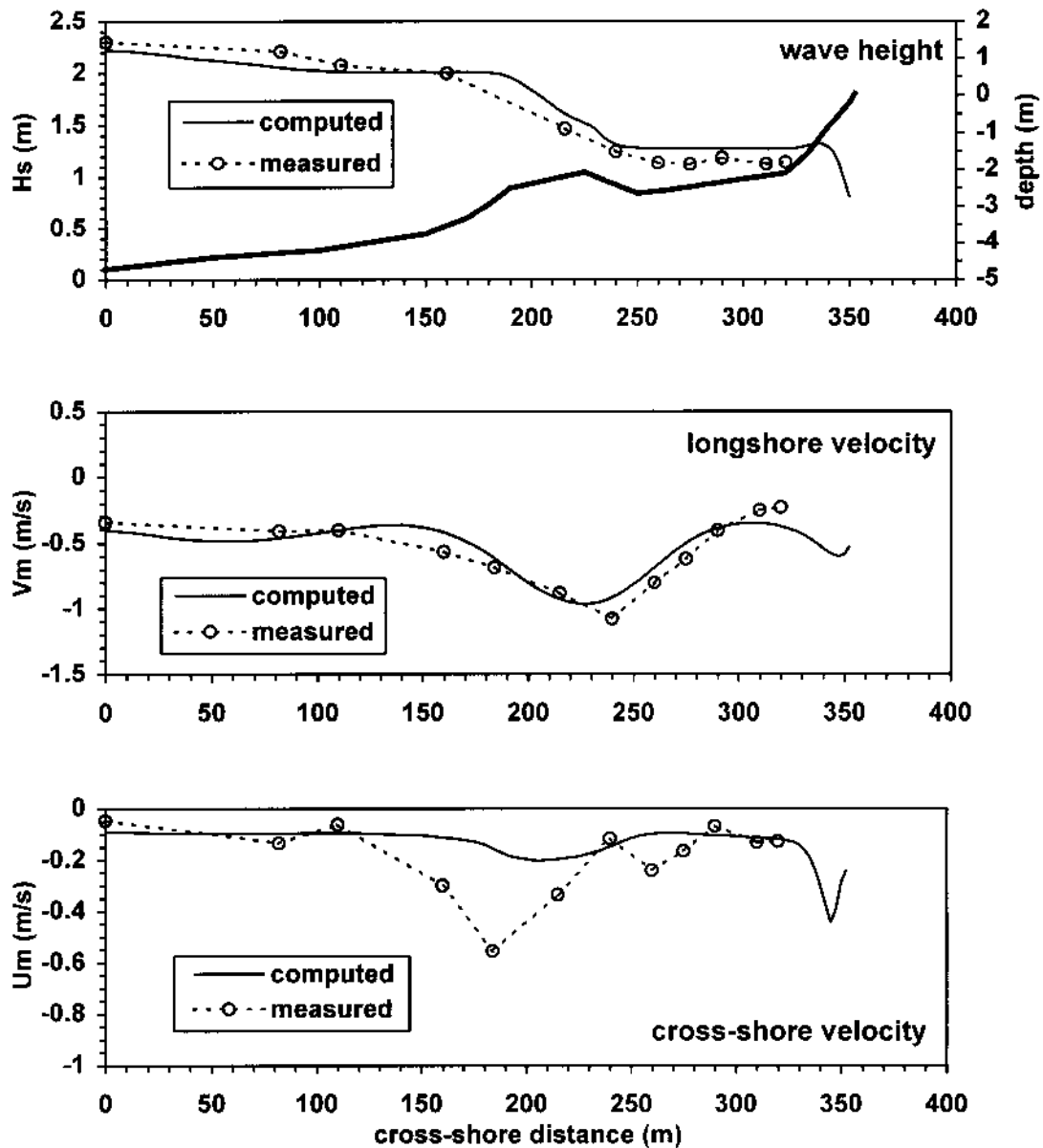


Figure 8. Example of measured and computed wave heights and time-averaged cross- and longshore velocities near Duck measured on 14 October 1994.

The measured and predicted cross-shore profile changes from 10-20 October are presented in Figures 9 and 10. Using an efficiency factor of $k = 0.2$ for the wave-related transport rates results in a predicted profile with three bars (Figure 9A): one near the shore, one just landward of the initial bar position and one more seaward. Decreasing the efficiency factor to $k = 0.05$ (Figure 9B) improves the predictions in the respect that: 1) the location of the outer bar ($x = 150$ m) agrees fairly well with the observed position, 2) the middle bar at $x = 250$ m is less pronounced and 3) the deposition of sand around $x = 320$ m is also seen in the measurements. The erosion of the region near the beach and in the offshore zone is not seen in the measured profile changes.

Next step was to locally enhance the undertow with a 'rip-factor' to give better agreement with the measured return flows. Figure 10A shows the measured profile and the predicted profile using $k = 0.2$. This figure illustrates that locally enhancing the undertow improves the model performance. The model reasonably predicts the overall profile changes. The offshore migration of the sand bar is somewhat too small.

Using an efficiency factor of $k = 0.05$ (Figure 10B) leads to a better prediction of the bar migration but the erosion near the beach ($x > 340$ m) and in the offshore region ($x < 100$) is too large in this case.

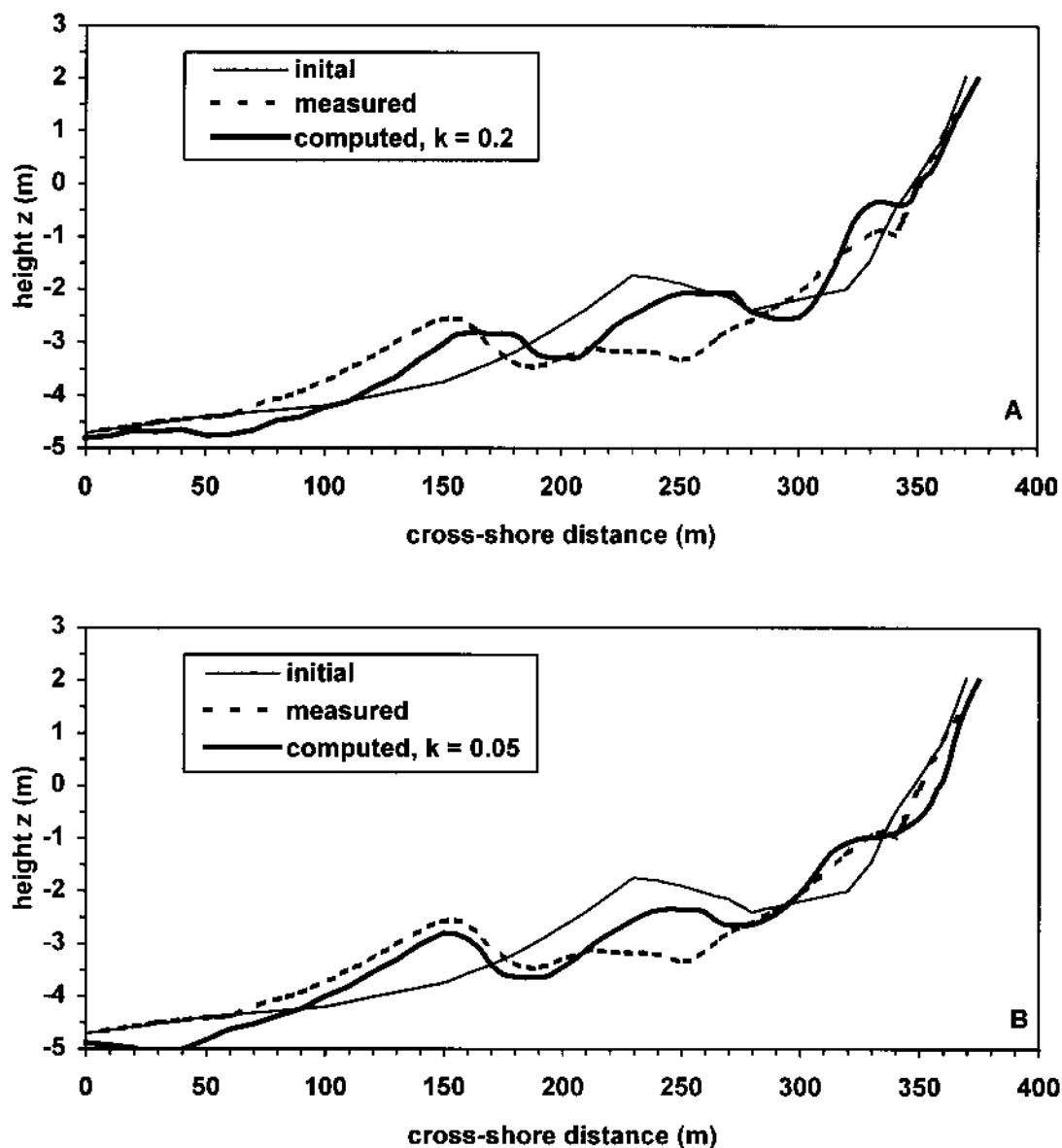


Figure 9. Measured and computed cross-shore profile changes near Duck from 10 to 20 October 1994.

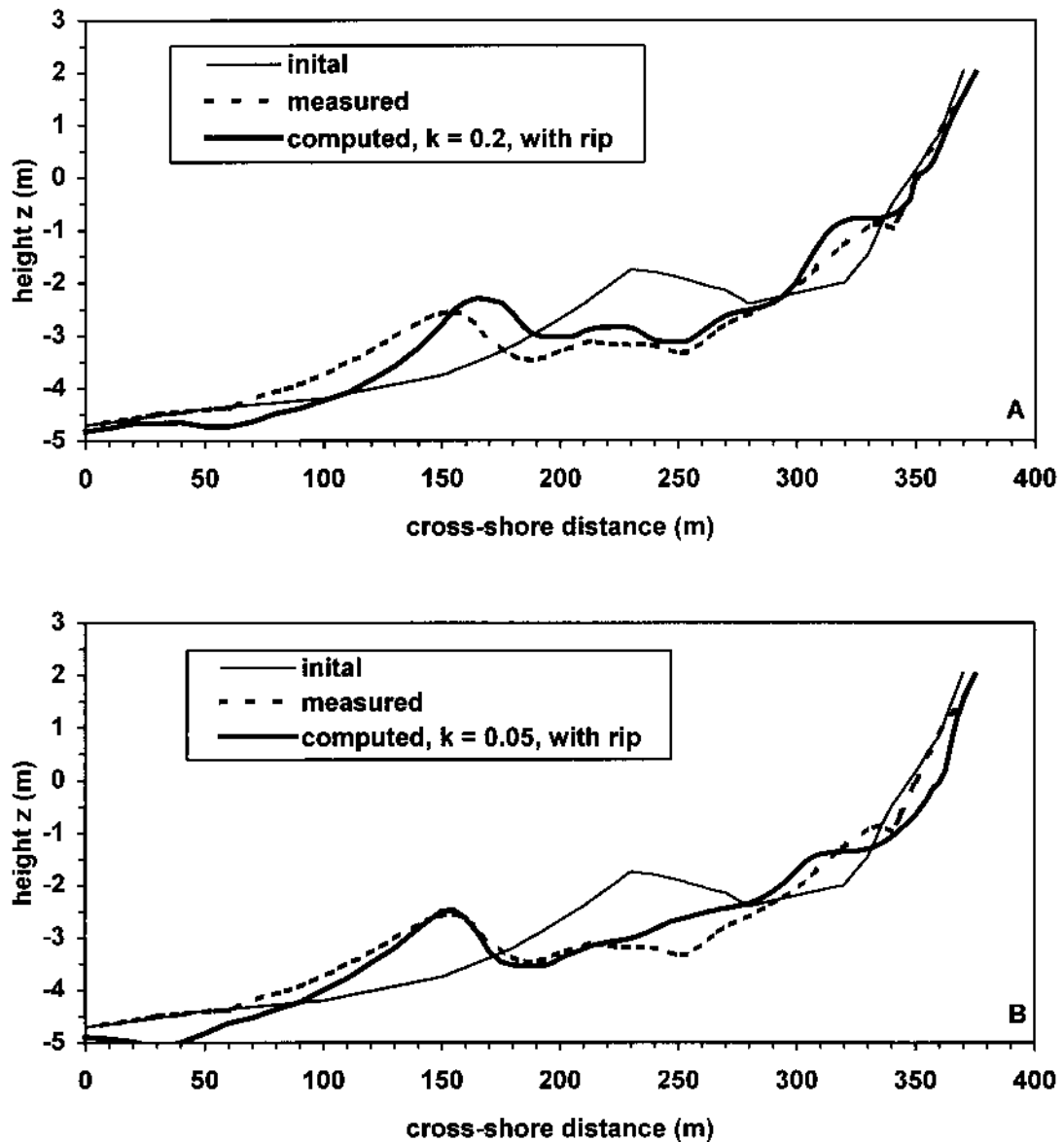


Figure 10. Measured and computed cross-shore profile changes near Duck from 10 to 20 October 1994. The cross-shore undertow was locally enhanced in the model to give better agreement with the measured returns flows.

It is interesting to see that increasing the undertow in agreement with the measured values also leads to a better prediction of the cross-shore morphological changes. This suggests that the offshore migration of the nearshore bar is a phenomenon related to cross-shore processes.

The large undertow velocities measured during the October event may be explained by the bathymetric map of the Duck site on 20 October 1994 in Figure 11. This figure shows the occurrence of significant longshore non-uniformities accounting for the presence a rip current.

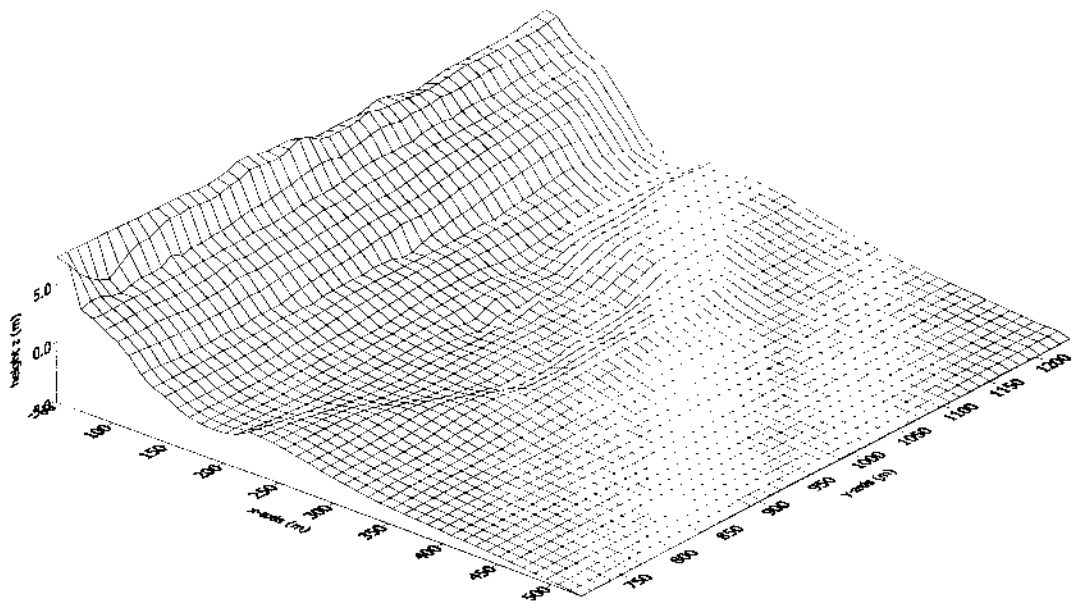


Figure 11. Local morphology near Duck, 20 October 1994.

5. CONCLUSIONS

The current-related suspended transport rates computed with the model based on the measured hydrodynamics near Egmond aan Zee could be predicted within a factor 2. A bed roughness height of $r_w = 0.02$ m gave the best results.

The measured wave-related suspended transport rates near Egmond aan Zee were on an average 4 times smaller than the current-related components. The computed wave-related transport rate depends on the efficiency coefficient k (see Eq.3), which is a measure for the coherence between the velocity and the concentration signal. Comparison of the measured wave-related transport rates near Egmond aan Zee with computed transports based on measured hydrodynamics showed that the efficiency factor for this site is about $k = 0.02$.

Two bar migration events were selected from the Duck94 experiments to compare the model computations with measured wave heights, currents and morphological changes. The model was used to simulate calm weather waves with onshore bar migration in the period 21-26 September and storm waves with offshore bar migration in the period 10-20 October 1994.

The computed wave heights showed favorable comparison to the measured values except in the trough region where the wave heights were overestimated with about 20%. The longshore currents were represented by the model, although the currents in the trough region were underestimated during the storm event in October. Large disparities were observed for the cross-shore currents. The presence of a rip current during the October event may have caused the calculations to significantly depart from the measurements.

Onshore bar migration during the September event was predicted by the model using an efficiency factor of $k = 0.2$, though the migration was smaller than measured. No

onshore migration was predicted when using an efficiency factor of $k = 0.05$. As regards the October event, artificially increasing the undertow according to the measured values resulted in a fairly good agreement between the measured and computed bed profiles.

The present results indicate that the comparison between measured and computed profile changes is difficult if the computations are based on one single cross-shore profile. It may be more appropriate to longshore average a number of cross-shore profiles. The longshore distance over which this averaging should take place depends on the degree of longshore uniformity. For the site near Duck this distance should be at least 500 m.

ACKNOWLEDGEMENTS

Support was provided by the US Office of Naval Research, the National Ocean Partnership Program, the National Research Council and the National Science Foundation. The Duck field observations were gathered in collaboration with R.T. Guza, T.H.C. Herbers, and B. Raubenheimer. Staff from the Center for Coastal Studies (Scripps Institution of Oceanography) and the Field Research Facility (US Army Corps of Engineers) provided excellent logistical support.

This work was undertaken as part of the Coast3D project funded by the European Commission's research program MAST under Contract Number MAS3-CT97-0086.

REFERENCES

- Gallagher, E.L., Elgar, S., Guza, R.T., 1998. Observations of sand bar evolution on a natural beach. *Journal of Geophysical Research*, Vol. 103, No. C02, pp. 3203-3215.
- Grasmeijer, B.T., Dang Huu Chung, Van Rijn, L.C., 1999. Depth-integrated sediment transport in the surf zone. *Proc. Coastal Sediments 1999*, pp. 325-340, ASCE, New York.
- Grasmeijer, B.T., Van Rijn, L.C., 1998. Breaker bar formation and migration. *Proc. Coastal Engineering 1998*, pp. 2750-2758, ASCE, New York.
- Houwman, K.T. and Ruessink, B.G., 1996. Cross-shore sediment transport mechanisms in the surfzone on a timescale of months to years, *Proc. Coastal Engineering 1996*, pp.4793-4806, ASCE, New York.
- Soulsby, R.L., 1998. Coastal Sediment Transport: the Coast3D project. *Proc. Coastal Engineering 1998*, pp. 2548-2558, ASCE, New York.